JOURNAL OF MATERIALS SCIENCE 32 (1997) 1531–1544

Structural order in $Ba(Zn_{1/3}Ta_{2/3})O_3$, $Ba(Zn_{1/3}Nb_{2/3})O_3$ and $Ba(Mg_{1/3}Ta_{2/3})O_3$ microwave dielectric ceramics

D. J. BARBER†, K. M. MOULDING, JI ZHOU*
Hong Kong University of Science and Technology, Clear Water Bay, Kowloon, Hong Kong

MAOQIANG LI
Institute of Advanced Ceramics, China Building Materials Academy, Guanzhuang, East Suburb, Beijing, People's Republic of China

The process and nature of structural ordering and the factors that influence them have been investigated in the microwave dielectric perovskites, barium zinc tantalate (BZT), barium zinc niobate (BZN), and barium magnesium tantalate (BMT), sintered at various temperatures. The samples were characterized mainly by X-ray powder diffraction and transmission electron microscopy. The results show that short-range 1 : 1 B-site order features strongly in the early stages of ordering in BZT and BZN, but it is extremely rare in BMT, for which most grains commence with 1 : 2 order. As sintering progresses, 1 : 1 order is replaced by 1 : 2 long-range order in BZT and by disorder in BZN. Orientational variants of the ordered domains within grains occur in similar numbers when order is fine-scale, but their distribution is less homogeneous in well-ordered samples. Local inhomogeneities in the degree of order within grains, which will affect dielectric properties, correlate with both residual non-stoichiometry and the presence of dislocations. Incompletely reacted starting materials which may persist to late stages of sintering can also strongly influence order. Anomalously large ordered domains at grain boundaries are attributed to grain-boundary migration accompanied by enhanced diffusion. The results indicate that with starting materials that are well-mixed and homogeneous at the nanoscale, tailoring of physical properties should be possible by controlling the type and degree of order through chemical composition.

1. Introduction

Barium zinc tantalate (BZT) and barium magnesium tantalate (BMT) are disorder–order perovskite-type oxide compounds. Pure barium zinc niobate (BZN) is classified as a disordered perovskite. All three compounds have the general formula $A^{2+}(B^{2+}_{1/3}\,B^{5+}_{2/3})O_3$. When disordered, they have cubic unit cells with $a_0 \sim 0.4095$ nm and symmetry $Pm\bar{3}m$. The ordered compounds adopt a trigonal symmetry owing to a rhombohedral distortion along a $\langle 1\,1\,1 \rangle$ direction of the cubic cell, together with a slight volume increase [1–4]. The trigonal symmetry is $P\bar{3}\,m\,1$ like that of $Ba(Sr_{1/3}Ta_{2/3})O_3$ [5], and the ordered compounds are indexed in terms of hexagonal unit cells with $a = 0.577$–0.578 nm and $c = 0.707$–0.709 nm. The three oxide compounds, BZT, BZN and BMT, are non-ferroelectric. They are of functional interest as microwave dielectric materials because they have high dielectric constants, very low dielectric losses (high Q-values), and low-temperature coefficients of their resonant frequencies [2, 6–10]. Ordering behaviour in microwave dielectrics has both fundamental and practical aspects, the latter being typified by the finding that Q-values depend on the degree of order [6, 9]. A relationship between dielectric microwave loss and the degree of order has been derived for BZT by Sagala and Nambu [11]. Such a dependence is not surprising. B-site order in perovskites has a profound influence on physical properties [9] and has been the subject of many investigations, e.g. [12–15]. Desu and O'Bryan [8] have demonstrated for BZT that ordering is very sensitive to processing conditions, and so similar behaviour might be anticipated for BMT, which is difficult to obtain disordered, but not for BZN (which is not reported to order).

2. Order transformations in compounds

Ordering mechanisms may be heterogeneous, homogeneous, or spinodal [16]. The heterogeneous reaction

† *Present address*: School of Industrial and Manufacturing Science, Cranfield University, Cranfield, Bedfordshire MK43 OAL, UK.
* *Permanent address*: Department of Materials Science and Engineering, Tsinghua University, Beijing, People's Republic of China.

0022–2461

involves the spontaneous onset of the ordering transformation within discrete microregions. It does not necessarily mean nucleation at crystal defects, as is generally implied when the term heterogeneous nucleation is used to describe the onset of solute segregation.

The ability of $A(B'B'')O_3$ perovskites to order depends mainly on the differences in size and valency of the two B-site ions: large differences in each property favour order. The order observed by X-ray and TEM methods [12–15, 17] in the lead-based (A = Pb) perovskites, which constitute the most widely studied group, can essentially be classified as domains of long-range order ranging from the nanoscale (~ 10 nm) to the microscale (>100 nm). The achievement of a high degree of order in all types of compounds which are predisposed to order requires the constituent atoms to be present in stoichiometric proportions. A further free-energy constraint is that ordering should not generate local charge imbalances. These are inevitable when an off-stoichiometric, partially ionic compound, orders. For example, problems of this nature are responsible for the inability of the ferroelectric, lead magnesium niobate, $Pb(Mg_{1/3}Nb_{2/3})O_3$ (PMN) to acquire more than a small degree of long-range order [18]. Ordering in PMN is promoted by replacing some Pb^{2+} with La^{3+}, and by moving the Mg : Nb ratio closer to 1 : 1 to maintain charge balance [19]. Non-stoichiometry in the same compound affects the ageing behaviour of the dielectric constant [20].

3. Ordering, Bragg reflections and diffraction contrast

The structure of the ordered unit cell of the $A^{2+}(B^{2+}_{1/3}\,B^{5+}_{2/3})O_3$ compounds, together with the pseudocubic cell, is illustrated in Fig. 1a. (The effect on stacking of the 1 : 2 ordering of the B-site cations is seen in Fig. 7c.) The degree of long-range structural order (LRO) can be measured by X-ray methods, and expressed in terms of the ratio of the intensity of a superstructure reflection to that of a basic unit cell reflection.

B-site 1 : 2 order in $AB''B''O_3$ compounds creates superlattice reflections in electron diffraction patterns which do not correspond to reciprocal lattice points for the fundamental perovskite cell with integer values $\{h, k, l\}$. It is convenient and common, however, to refer to a pseudo-cubic unit cell when describing diffraction data from ordered perovskites. Thus, in addition to the strong intensity maxima at allowed $\{h, k, l\}$ positions, weaker maxima occur at $\{h \pm \frac{1}{3},\ k \pm \frac{1}{3},\ l \pm \frac{1}{3}\}$. (These correspond to reflections like $1\,0\,\bar{1}\,0$, $1\,0\,\bar{1}\,1$ when indexing is in terms of the hexagonal cell.) Short-range order (SRO) is manifest as diffuse intensities at or through the positions of order reflections and arcing of the spots corresponding to basis reflections. A ring of diffuse intensity probably denotes a transition from SRO to LRO, as found with other materials systems [21].

In perovskites that undergo 1 : 1 B-site ordering, the unit cell has edges of length double that of the basic perovskite unit cell, resulting in superlattice reflections

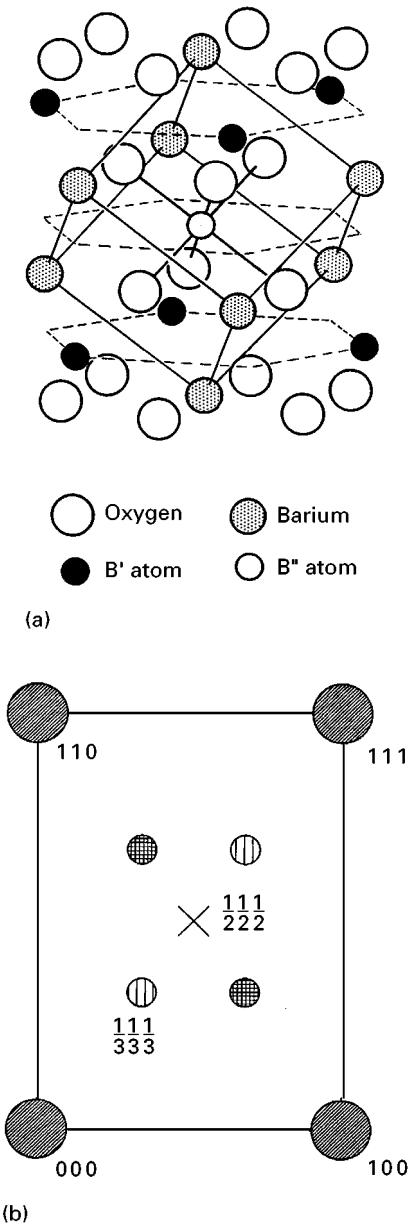

Figure 1 (a) Schematic illustration of the 1 : 2 ordered structure of an $A(B'_{1/2}\,B''_{2/3})O_3$ perovskite. The rhombohedral distortion of the cell is not shown. (b) Schematic illustration of a $[1\,\bar{1}\,0]$ zone electron diffraction pattern, illustrating the positions of the base and non-base lattice reflections in a single cell of the reciprocal lattice, indexed in terms of the perovskite cubic pseudo-cell. Intensity at the $\{h \pm \frac{1}{2},\ k \pm \frac{1}{2},\ l \pm \frac{1}{2}\}$ positions can arise from either 1 : 1 B-site atomic order or antiphase oxygen-cage tilting. Any intensity at the $\{h \pm \frac{1}{3},\ k \pm \frac{1}{3},\ l \pm \frac{1}{3}\}$ positions arises solely from 1 : 2 B-site atomic order. The reflections denoted by the small square-hatched circles may arise from double diffraction.

that occur at the positions $\{h \pm \frac{1}{2},\ k \pm \frac{1}{2},\ l \pm \frac{1}{2}\}$. A further point of possible relevance is that for perovskites which have tilted oxygen cages [22, 23] and can therefore have orientational variants with oxygen cages that are tilted in antiphase, the lowest-order reflections with this origin are $\{\frac{3}{2}, \frac{1}{2}, \frac{1}{2}\}$. The dynamical diffraction conditions which readily occur in TEM and cause double diffraction means that $\{\frac{3}{2}, \frac{1}{2}, \frac{1}{2}\}$ reflections also appear at positions $\{\frac{1}{2}, \frac{1}{2}, \frac{1}{2}\}$ etc. Thus $\{h \pm \frac{1}{2},\ k \pm \frac{1}{2},\ l \pm \frac{1}{2}\}$ reflections can either arise solely from or have a contribution from oxygen-cage tilting. They are not necessarily just an indication of B-site

order. Reaney *et al.* [24] have recently correlated the occurrence of oxygen-cage tilting with tolerance factor (which is a measure of the relative sizes of ions, used by Megaw to discuss the stability of the perovskite phase [25]). The compounds BMT and BZN do not undergo oxygen-cage tilting, because they have tolerance factors > 0.985 [24]. However, calculation shows that BZT has a tolerance factor < 0.97 and therefore it belongs to a group of compounds that undergo antiphase tilting. BZN does not order, according to the literature, although ordering occurs in barium-poor members of the solid-solution series incorporating strontium zinc niobate and these mixed perovskites also exhibit evidence of oxygen-cage tilting [26, 27].

In order to facilitate understanding and for ease of comparison, we illustrate mostly electron diffraction patterns with $\langle 1\,1\,0 \rangle$ zone axes for which the superlattice reflections for 1 : 2 (i.e. stoichiometric) order should occur at $\frac{1}{3}$ and $\frac{2}{3}$ along the diagonals of the rectangle that is a $\langle 1\,1\,0 \rangle$ projection of the reciprocal cell for the base lattice, Fig. 1b. Any reflections corresponding to 1 : 1 order would occur at the centre of the cell, coincident with positions of so-called α-reflections [24] caused by antiphase tilting.

Domains and domain boundaries produced by ordering transformations can be directly imaged by TEM methods. Domains are related by the point group symmetry elements lost on ordering and thus they may be either translational or orientational variants, generally with equal probabilities of occurrence. Ideal domain boundaries deriving from the transformation of the cubic disordered perovskite will therefore be either antiphase boundaries (APBs), characterized by a constant displacement vector, or twin boundaries (TBs). In reality, boundaries of mixed character may occur. The different variants are not easy to identify in weakly ordered materials where the domain size is small. In well-ordered compounds the twin-related domains are easily recognized because TBs separate areas which exhibit different diffraction contrast for most operating reflections. Displacement-related domains do not show differences in diffraction contrast. By applying diffraction conditions in the TEM, and particularly by imaging in dark-field with specific order reflections, both the nature of order and the relationships between ordered regions can be analysed.

4. Experimental procedure

The ceramics were made by the sintering of homogenized mixtures of powders. For simplicity of identification, we refer to samples by a shorthand form, e.g. BZT15 is a barium zinc tantalate sample that has been sintered at 1500 °C. Zinc, niobium and tantalum oxides and the carbonates, $BaCO_3$ and $Mg(OH)_2 \cdot 4MgCO_3 \cdot 4H_2O$, were used as precursors for making ceramic powders using the following route: appropriate amounts of oxides or carbonates were weighed according to the stoichiometry of $A(B'_{1/3}B''_{2/3})O_3$, they were mixed in an alumina jar with zirconia balls and ethanol for 24 h, the resulting slurry was dried, followed by calcining at 1300 °C for 2 h. The calcined powders were then separately ball-milled with zirconia balls and ethanol. After further drying, the powders were uniaxially pressed into pills, and sintered at various temperatures for 2 h (except for BMT14, BMT15 and BMT16, which were held at the sintering temperature for 10 h). The resulting materials were characterized by powder diffraction, density, micro-Raman spectroscopy (for BMT only) and transmission electron microscopy (TEM). The dielectric constants and dielectric losses of BMT samples were measured in the millimetre band by a quasi-optical technique.

TEM specimens were made by cutting slices from the sintered drums, lapping and polishing to form thin sections, and then ion milling these in standard fashion. TEM investigations were carried out with a Philips CM20 microscope fitted with a double-tilt specimen holder and a windowless energy dispersive X-ray detector, supported with Isis microanalysis software (Oxford Instruments). A Gatan liquid-nitrogen-cooled double-tilt holder was used for some experiments. Imaging, diffraction and microanalysis were all performed at 200 kV.

5. Characteristics of sintered samples

Measurements of the apparent densities of the BMT samples are as shown in Table I. The density of BMT16 is less than that of BMT15, probably because of fast grain growth in the former, which can result in the microfractures and voids, or in the formation of second phase [28]. Comparable changes in density with sintering temperature occurred in the other two compounds. The dielectric properties were measured for a BMT sample sintered at 1550 °C for 2 h. At a frequency of 6.9 GHz, the dielectric constant was 24.98 and the Q-value was 5000. At 35 GHz, the dielectric constant was 23.23 and the Q-value was 1497. No such measurements were made on BZT and BZN.

6. Observations concerning structural order

6.1. Results from X-ray diffraction

X-ray powder diffraction results for the three compounds show differences in ordering behaviour that are broadly in accord with expectations. Comparing

TABLE I

Sample	Density (g cm^{-3})
BZT13	6.20
BZT14	7.41
BZT15	7.44
BZN13	5.79
BZN14	5.95
BZN15	5.96
BMT13	5.68
BMT14	5.75
BMT15	7.21
BMT16	6.93

the data for samples sintered at 1400 °C, the diffraction peaks show that order is only evident for the BMT sample. Using the ratios of line intensities, the results show that the degree of order in BMT increases with the temperature of sintering. The superlattice reflections (referred to the cubic pseudocell) are of the type $\{h \pm \frac{1}{3}, k \pm \frac{1}{3}, l \pm \frac{1}{3}\}$, which are characteristic of the 1 : 2 ordered trigonal structure. There is no weak peak for BMT at 0.4722 nm which would correspond to a $\{\frac{1}{2}, \frac{1}{2}, \frac{1}{2}\}$ reflection. There was no clear evidence for ordering in BMT powder calcined at 1300 °C for 4 h. However, this does not imply lack of order, and TEM shows that the ordered regions are very small (see Section 6.2.3) so that they would only give very diffuse X-ray peaks, easily lost in the background.

No indication or ordering is present in the X-ray results for BZN, Fig. 2a. For sintered BZT, peaks only occur which correspond to the 1 : 2 order reflections, Fig. 2b.

6.2. Results from transmission electron microscopy

6.2.1. Barium zinc tantalate

TEM methods are more sensitive for detecting the onset of ordering than X-ray diffraction. That ordering has started in BZT13, the least-sintered sample, is indicated by a nanoscale domain structure in some grains. The sample has a huge range of grain sizes, with many very small grains ($\sim$0.1 μm diameter) on the peripheries of larger ones (average grain size $\sim$1 μm). Order is at once apparent in the larger grains because many of them exhibit a finely dappled microstructure, caused by domains, $\sim$1 nm diameter. (The term "dappled" is used for choice, to make some distinction from the appearance of ferroelectric microdomains in $A(B'B'')O_3$ perovskites, which are often described as endowing grains with a mottled appearance.) Of course the ordered microstructures have their counterparts as superlattice spots in the corresponding selected-area diffraction patterns (SADs).

A significant proportion of grains in BZT13 give $\langle 1\,1\,0 \rangle$ SADs with weak spots at the centres of diffuse crosses whose arms are streaks of intensity extending along the cell diagonals towards the nearest $h\,k\,l$ positions, Fig. 3a. In principle, this could indicate either 1 : 1 SRO or antiphase oxygen cage tilting [26]. However, the former is our favoured explanation, because there is no sign that the $\{h \pm \frac{1}{2}, k \pm \frac{1}{2}, l \pm \frac{1}{2}\}$ become sharper or increase in intensity, relative to base lattice reflections, when such specimens are cooled to liquid-nitrogen temperature. (The intensities of order reflections should not alter, but those due to antiphase tilting should increase with decreasing temperature because the angle of tilt increases.) Diffraction patterns show that 1 : 2 order is absent or very weak in BZT13, at the most being witnessed by somewhat increased intensity of the diffuse streaking at the $\frac{1}{3}$ and $\frac{2}{3}$ positions (1 : 2 SRO).

Sample BZT14 appears to be generally less ordered than BZT13, but the grain size in the former is larger and more uniform. It appears that the mechanism responsible for the $\{\frac{1}{2}, \frac{1}{2}, \frac{1}{2}\}$-type spots (which we attribute to incipient 1 : 1 ordering) and found extensively with BZT13, is not favoured by grain growth. Grains giving such reflections were still evident in BZT14, Fig. 3b, but most SADs were indicative of 1 : 2 order. The domain size varied from grain to grain. It was typically 3–5 nm, but in some grains domains as large as 10 nm occurred. Comparison of the differences in the distribution of diffuse intensity between base-lattice spots in SADs from BZT14 and BZT13 suggests development towards 1 : 2 SRO in the former even where 1 : 1 order occurs.

The grain size in BZT15 was 2–5 μm and the domain size was much larger than in BZT14, being $\sim$50 nm. Most SADs indicated 1 : 2 order, with well-defined superlattice spots. Patterns from some grains still exhibited very weak and diffuse "crosses" through the $\{h \pm \frac{1}{2}, k \pm \frac{1}{2}, l \pm \frac{1}{2}\}$ positions, Fig. 3c. We deduce that the 1 : 2 domain variants are present in similar proportions because all the diffraction patterns appear to show the presence of twins. In zone axis patterns this could result simply from double diffraction because the specimens are thick enough to give dynamical effects. But the twin-related superlattice spots persist and do not change much in intensity when a grain is tilted away from a zone axis orientation.

We used microanalysis in an attempt to examine whether a compositional trend such as a paucity of the B″ element could explain the 1 : 1 order in BZT, but no trend was apparent. The 1 : 1 ordered grains found in all the samples were slightly off stoichiometry , but not in a systematic manner.

6.2.2. Barium zinc niobate

Many grains in BZN13 display fine-scale dappled (ordered domain) microstructures. These varied in scale by a factor of about five and were generally coarser in small grains than in the larger ones, Fig. 4a. Larger domains also often occurred near the boundaries of larger grains and their location sometimes appeared to mark the earlier positions of fine-grained inter-particulate materials, Fig. 4b. The SADs from such dappled grains exhibited intensity at superlattice positions, but experience showed that this could be strongest and sharpest at either the (cubic pseudocell) 1 : 1 superlattice positions $\{h \pm \frac{1}{2}, k \pm \frac{1}{2}, l \pm \frac{1}{2}\}$, and/or at the 1 : 2 superlattice $\{h \pm \frac{1}{3}, k \pm \frac{1}{3}, l \pm \frac{1}{3}\}$ positions; Fig. 5a illustrates both occurring together. SADs from other grains indexed simply in terms of the basic perovskite unit cell but show some very diffuse streaked intensities. We conclude from these results that there are many grains with SRO, of both 1 : 1 and 1 : 2 type, and some with LRO, although this tends to be of 1 : 2 type.

Many grains in BZN14 did not give distinct superlattice spots, even with weak intensities. A careful search produced a few instances where there were discernable spots with streaking, of which Fig. 5b is an example. Such patterns required a long exposure to reveal the $\{h \pm \frac{1}{2}, k \pm \frac{1}{2}, l \pm \frac{1}{2}\}$-type spots, which is why the base spots appear so large. Note the diffuse ring almost through the 1 1 0 positions. This ring

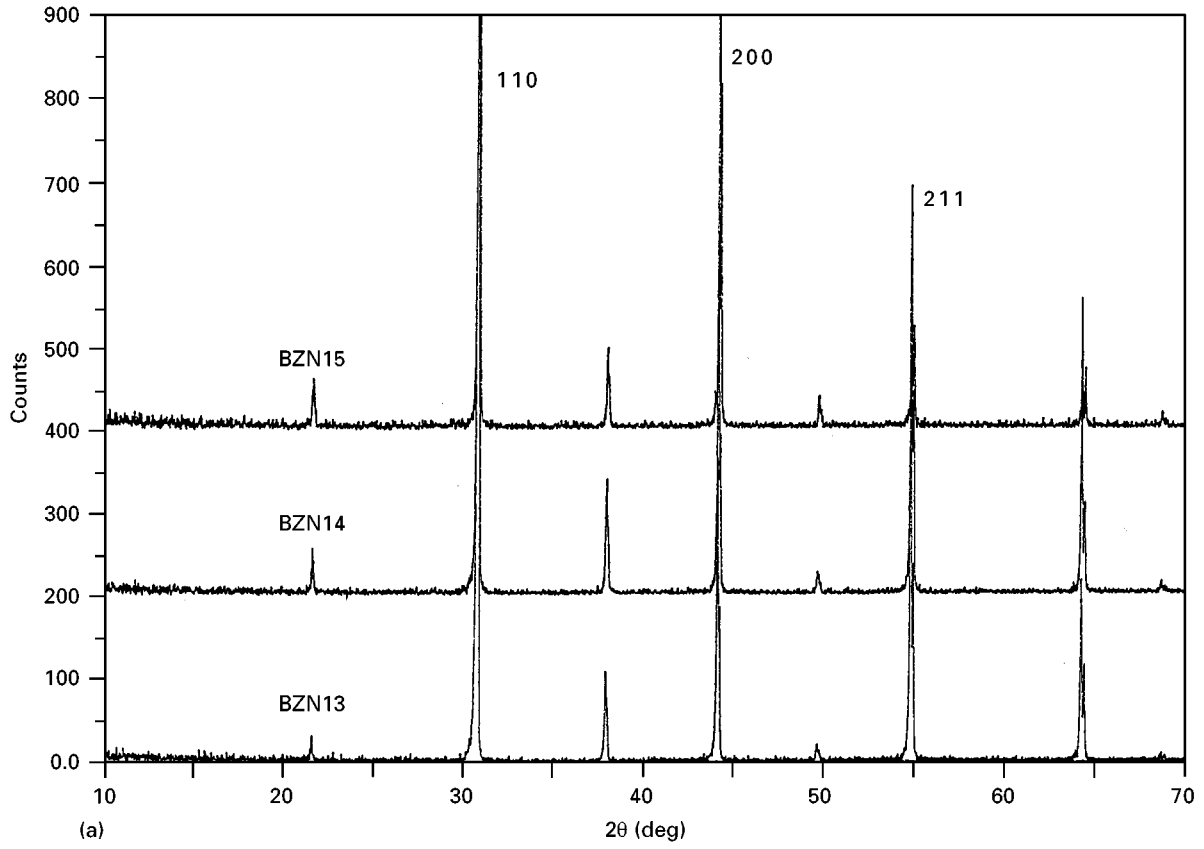

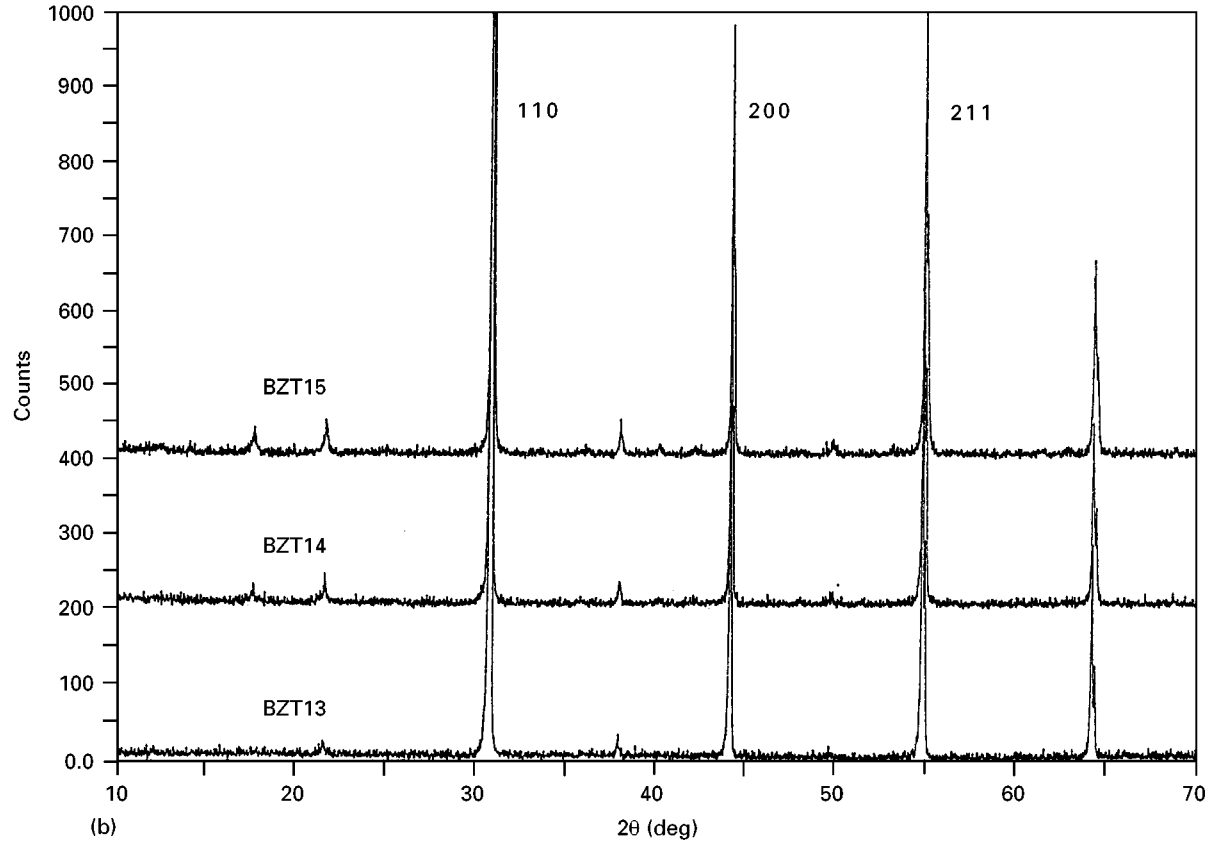

Figure 2 X-ray powder diffraction results from the ceramics after sintering at various temperatures: (a) BZN, (b) BZT. Reflections of type $\{h \pm \frac{1}{2}, k \pm \frac{1}{2}, l \pm \frac{1}{2}\}$ are not apparent in either of the records, but weak reflections of the $\{h \pm \frac{1}{3}, k \pm \frac{1}{3}, l \pm \frac{1}{3}\}$ type are visible in the results for barium zinc tantalate sintered at 1500 °C.

appeared in SADs from about 10% of the grains, often with arcing through the base reflections and occasionally with weak intensity at the $\{\pm\frac{1}{2}, \pm\frac{1}{2}, \pm\frac{1}{2}\}$ positions in $\langle 1\,1\,0 \rangle$ SADs, as illustrated in Fig. 5c. Such features indicate that some transitional SRO is present. The same grains have an extremely fine-scale dappled microstructure. The grain structure is better developed in BZN14 than in BZN13 and there

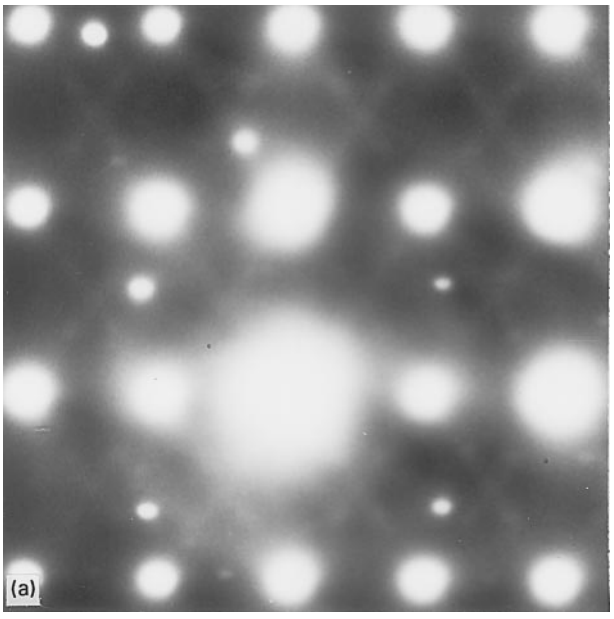

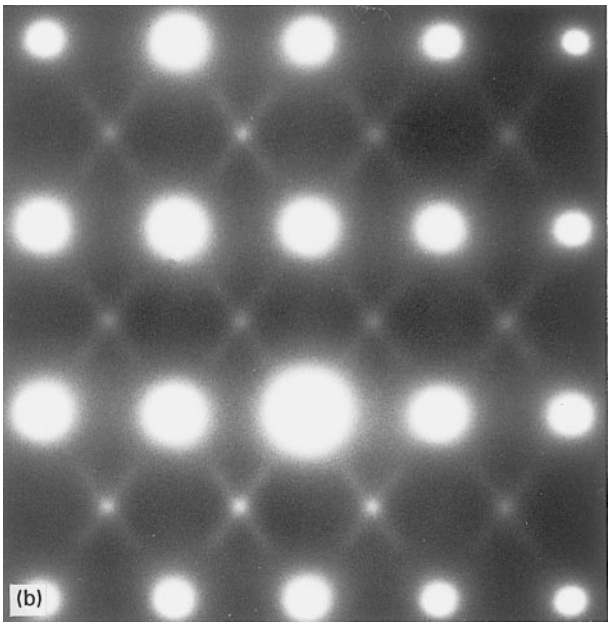

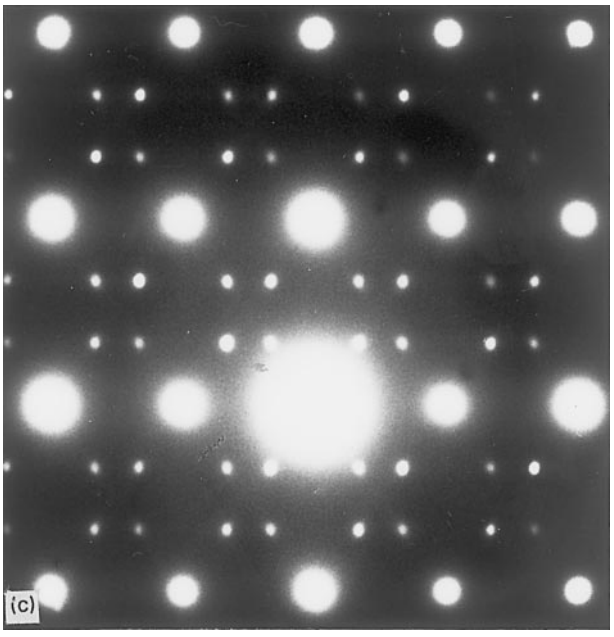

Figure 3 $\langle 1\,1\,0 \rangle$ zone axis electron diffraction patterns from BZT samples showing intensity at the $\{h \pm \frac{1}{2}, k \pm \frac{1}{2}, l \pm \frac{1}{2}\}$ and/or the $\{h \pm \frac{1}{3}, k \pm \frac{1}{3}, l \pm \frac{1}{3}\}$ order reflection positions: (a) BZT13, (b) BZT14, (c) BZT15. A long exposure was needed to reveal the diffuse intensities in (a), and the extra reflections come from a neighbouring grain.

appears to be less compositional inhomogeneity, which probably explains the lesser extent of 1 : 1 ordering (see Section 7).

For BZN15 the grain structure is well equilibrated. The diffraction patterns again vary from grain to grain, and the specimens seem more like BZN13 as regards structural order. Some $\langle 1\,1\,0 \rangle$ zone axis patterns have distinct spots of low intensity at the $\{h \pm \frac{1}{2}, k \pm \frac{1}{2}, l \pm \frac{1}{2}\}$ positions with diffuse streaking through them extending towards the nearest $h\,k\,l$ positions. Other $\langle 1\,1\,0 \rangle$ SADs have different distributions of diffuse intensity, with weaker isolated spots at $\{h \pm \frac{1}{2}, k \pm \frac{1}{2}, l \pm \frac{1}{2}\}$ or with the diffuse streaks concentrated

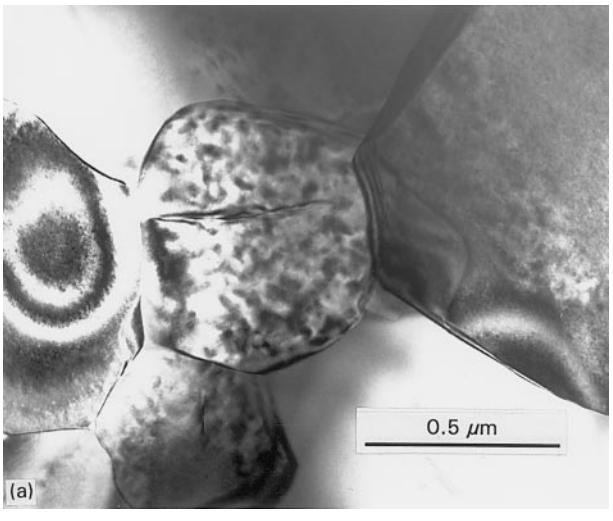

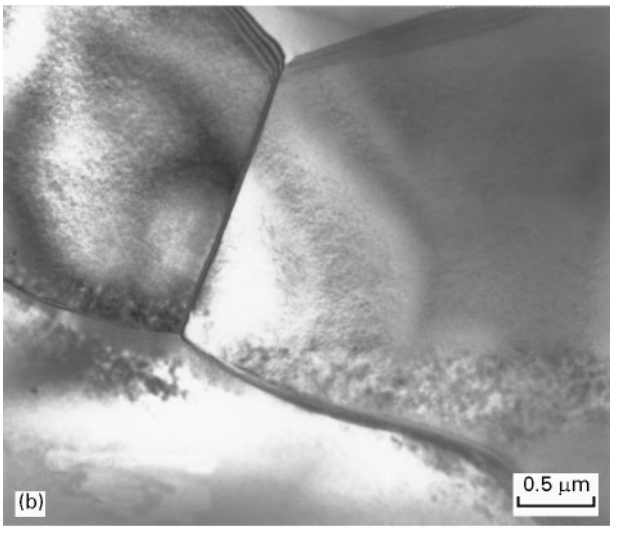

Figure 4 Micrographs showing the variation of sizes of order domains in BZN13: (a) apparent influence of grain size, (b) apparent influence of migration of grain boundaries and earlier presence of fine-grained particulate.

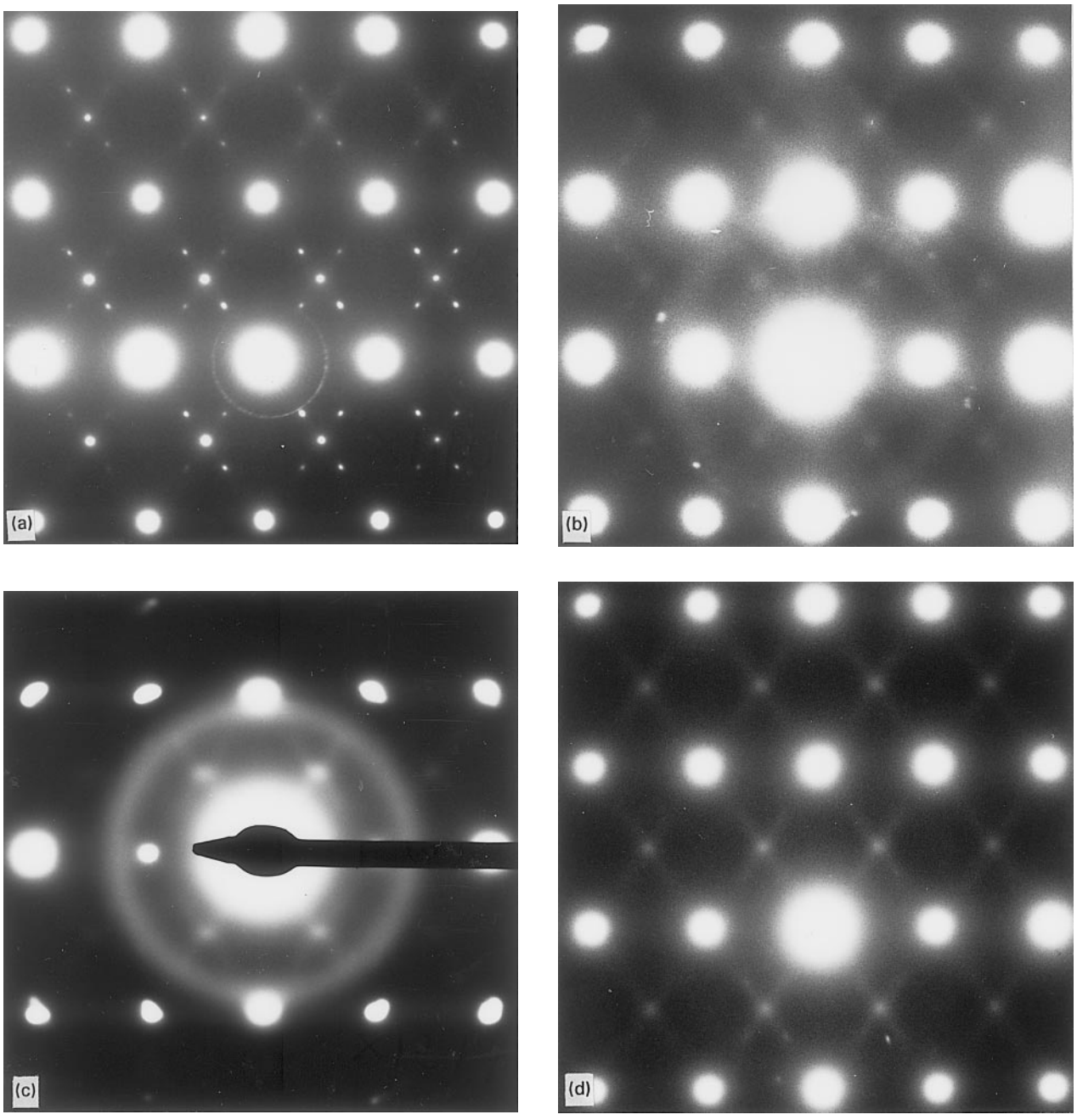

Figure 5 ⟨1 1 0⟩ zone axis electron diffraction patterns from BZN samples: intensity at the $\{h \pm \frac{1}{2}, k \pm \frac{1}{2}, l \pm \frac{1}{2}\}$ positions in (a) BZN13, (b) BZN14, (c) BZN14, (d) BZN15. In (a) $\{h \pm \frac{1}{3}, k \pm \frac{1}{3}, l \pm \frac{1}{3}\}$ spots are also present, while (c) illustrates arcing of base reflections and a stronger diffuse ring.

into spots through the $\{h \pm \frac{1}{3}, k \pm \frac{1}{3}, l \pm \frac{1}{3}\}$ positions, Fig. 5d, which are sometimes slightly elongated. For the grains which exhibit only 1 : 2 ordering (the majority) the reflections occur which correspond to the two twin variants that should show in the ⟨1 1 0⟩ patterns. The reflections for the twin variants still appear in diffraction patterns after tilting off the zone axis, showing that the variants are indeed present among the fine-scale ordered domains and in roughly equal numbers. Domain sizes were ∼5 nm in BZN13, 10 nm in BZN14 and ∼25 nm in BZN15.

6.2.3. Barium magnesium tantalate

The TEM results on ordering in specimens of BMT sintered at different temperatures are generally consistent with the X-ray results. Domains of order are present in all samples and their average size increases with the sintering temperature. The domain sizes are variable and less uniform the higher is the temperature; in BMT15 and BMT16 they are of the order of the grain sizes (∼1–5 μm). The superlattice (order) reflections in SADs occur at reciprocal lattice positions corresponding to $\{h \pm \frac{1}{3}, k \pm \frac{1}{3}, l \pm \frac{1}{3}\}$, confirming that most grains in all the samples conform to the trigonal structure. The domains in BMT15 and BMT16 have wider ranges of size, from ∼0.1–2 μm and ∼0.2–5 μm respectively, the upper limit being the grain scale in both cases. The domain size in BMT14 is 5–30 nm (the lower values applying in most grains) and the grain size is ∼0.1 μm. We also noted that in some ⟨1 1 0⟩ diffraction patterns from BMT14

there was a tendency for the 1:2 order reflections to be elongated along the diagonals of the reciprocal cell.

As a consequence of the findings on BZT and BZN, a search for evidence of 1:1 B-site order was made on BMT, carried out by examining $\langle 1\,1\,0 \rangle$ diffraction patterns wherever possible. No evidence was found for BMT15 and BMT16. Sample BMT14 was judged to be the most likely candidate of those available (it was not practical to work with samples sintered at a lower temperature). Because of the small grain size of BMT14, it was often difficult to isolate single grains by the selected-area diffraction method and microdiffraction was therefore widely used. In a few BMT14 diffraction patterns it was noticed that rings of weak diffuse intensity passed almost through the 1 1 0 positions, and there was sometimes perceptable arcing of the base spots. Very rarely were grains found that generated no $\{h \pm \frac{1}{3}, k \pm \frac{1}{3}, l \pm \frac{1}{3}\}$ superlattice spots. Instead they gave very faint diffuse streaks of intensity through the $\{h \pm \frac{1}{2}, k \pm \frac{1}{2}, l \pm \frac{1}{2}\}$ positions in long-exposure $\langle 1\,1\,0 \rangle$ zone axis diffraction patterns, always with the diffuse ring and sometimes with slight arcing of the base reflections. An example is shown in Fig. 6. During printing the centre of this SAD has been exposed some four times more than the outer regions in order to reveal the weak $\{\pm\frac{1}{2}, \pm\frac{1}{2}, \pm\frac{1}{2}\}$ spots and the diffuse ring outside them. As in the case of BZN14 (Fig. 5b), this SAD indicates the presence of weak short-range 1:1 order (1:1 SRO). It shows that 1:1 order is possible in BMT, although transitional at 1400 °C and essentially absent in the samples sintered at higher temperatures.

One surprising TEM result was the discovery of a population of grains of fairly pure magnesium oxide ($< 4\%$ [Ba + Ta]), Fig. 7, in all the BMT samples. These MgO grains are readily apparent because they give less electron scattering and less absorption than the grains containing barium and tantalum. Their identity was established by electron diffraction, Fig. 7 (inset), and energy dispersive microanalysis. The grains of BMT surrounding the MgO show no marked departure from the average BMT composition

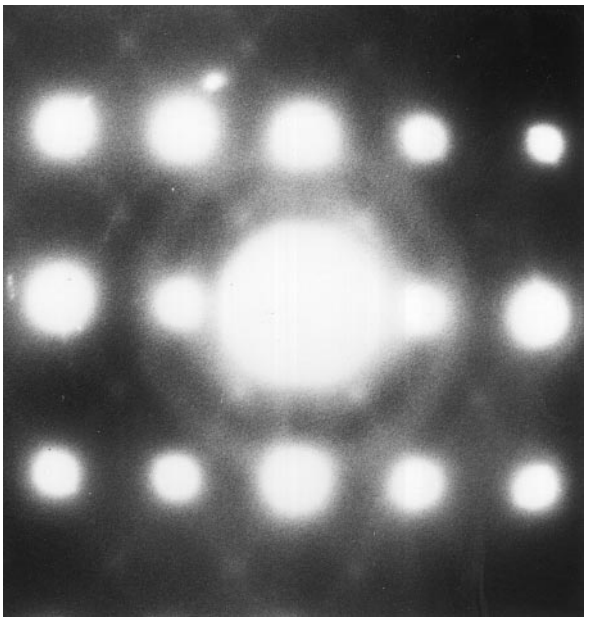

Figure 6 $\langle 1\,1\,0 \rangle$ zone axis electron diffraction pattern from BMT14, showing weak intensity at the $\{h \pm \frac{1}{2}, k \pm \frac{1}{2}, l \pm \frac{1}{2}\}$ positions and a diffuse ring of intensity passing close to the $\{1\,1\,0\}$ positions, which together indicate transitional 1:1 short-range order. During printing the centre of the pattern was exposed approximately four times more than the outer regions in order to reveal the weak $\{\pm\frac{1}{2}, \pm\frac{1}{2}, \pm\frac{1}{2}\}$ spots within the diffuse ring.

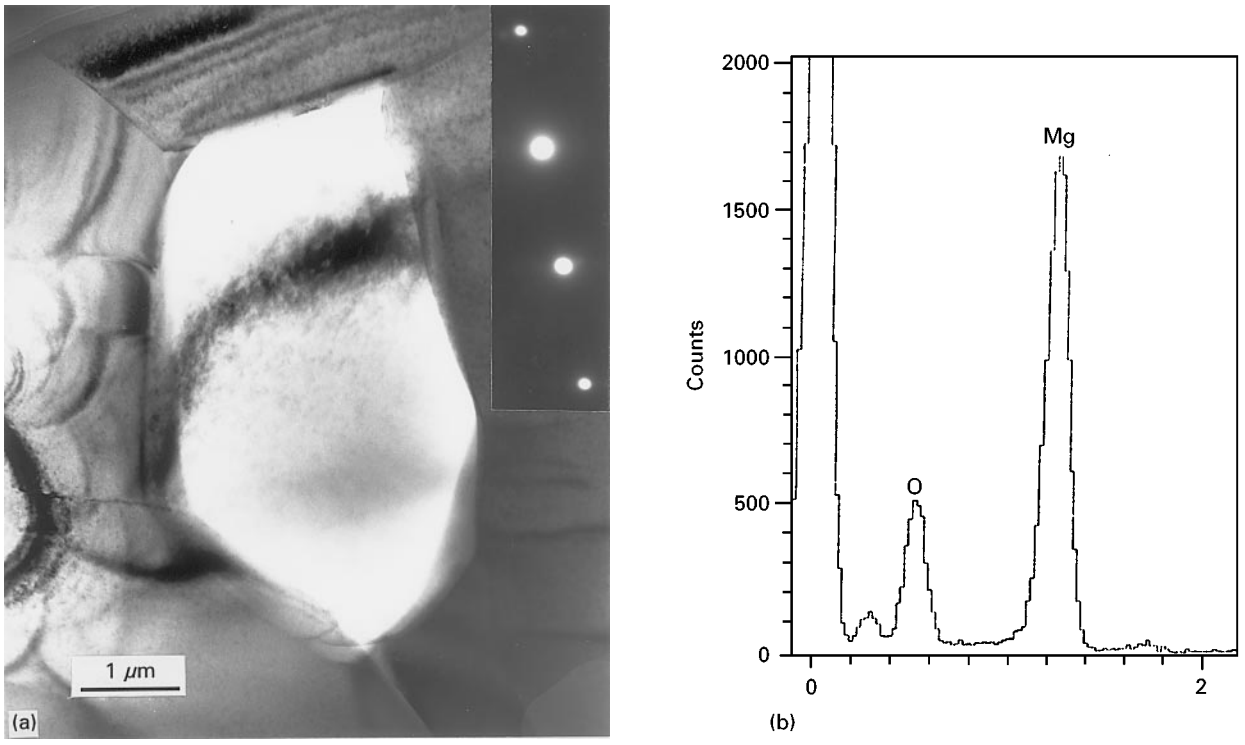

Figure 7 (a) Micrograph of an MgO grain in BMT16 with SAD (inset) and (b) EDX microanalysis spectrum from the grain.

and we did not discover any third phase. We therefore assume that the BMT in each of the samples is magnesium-poor, with the deficiency incorporated in some structural manner, possibly according to the formula $Ba(Mg_{(1-x)/3x/3}Ta_{2/3})O_3$. The occurrence of MgO grains decreased with sintering temperature and we anticipate that it will also decrease with sintering time, although we have not proved this. We doubt that the MgO in our sintered BMT ceramics is unique. This raises the question whether the reported changes in dielectric loss in BMT as a function of sintering temperature are not simply related to the degree of order, but may also have a contribution from MgO second phase.

(*Note added in proof*: The authors have identified rare grains of ZnO in the BZT and BZN ceramics which were sintered at low temperatures.)

6.3. Twin boundaries and antiphase boundaries in 1 : 2 ordered compounds

The results in this section mostly derive from BMT16 which is well sintered and fully ordered. The findings are fairly general and should apply to any of the barium and strontium-based perovskites that undergo 1 : 2 ordering. Here it is convenient to discuss diffraction patterns on a different basis, with indexing in terms of the hexagonal ordered cell.

Fig. 8a shows a $\langle 1\,1\,\bar{2}\,3\rangle$ zone axis SAD (corresponding to $\langle 1\,1\,0\rangle$ for the cubic pseudocell) from a grain in BMT16 which consists of just a few domains, none of which are twin-related variants. The curved interfaces between the domains show α-fringe contrast, indicating that they are antiphase boundaries (APBs) across which there is a displacement. (The interface produces a change in phase factor, $\alpha = 2\pi \boldsymbol{gR}$ where $\boldsymbol{g}$ is reciprocal lattice vector of the operating reflection, and $\boldsymbol{R}$ is the displacement across the interface.) The fringes of these interfaces are symmetrical in both bright and dark field, indicating that $\alpha = \pi$. The APBs are not confined crystallographically and normally they are characteristically curved, Fig. 8b. The idealized structure close to the APB is indicated by Fig. 8c.

Other types of domain boundary also occur, as expected. The diffraction pattern in Fig. 9a is the superposition of two $\langle 0\,1\,\bar{1}\,1\rangle$ zone axis patterns, one a reflection of the other across a $\{1\,0\,\bar{1}\,1\}$ plane, (a $\{1\,1\,1\}$ plane of the pseudocubic cell). These arise from the presence of domain interfaces that are twin boundaries (TBs). Ordering TBs are easily recognized in practice on account of differences in contrast between the domains on either side. The interfaces between the domains apparently have higher energy than displacement-related APBs because they favour low-index planes, as shown in Fig. 9b, and often zigzag from one to another. The fringe contrast shown by such an ordering twin interface, when tilted with respect to the electron beam, is consistent with expectations for TBs, i.e. the fringes are asymmetric in bright field. The atomic arrangement for twin-related domains is represented schematically in Fig. 9c, with $\{1\,0\,\bar{1}\,1\}$ being shown as both the twinning plane and the composition plane.

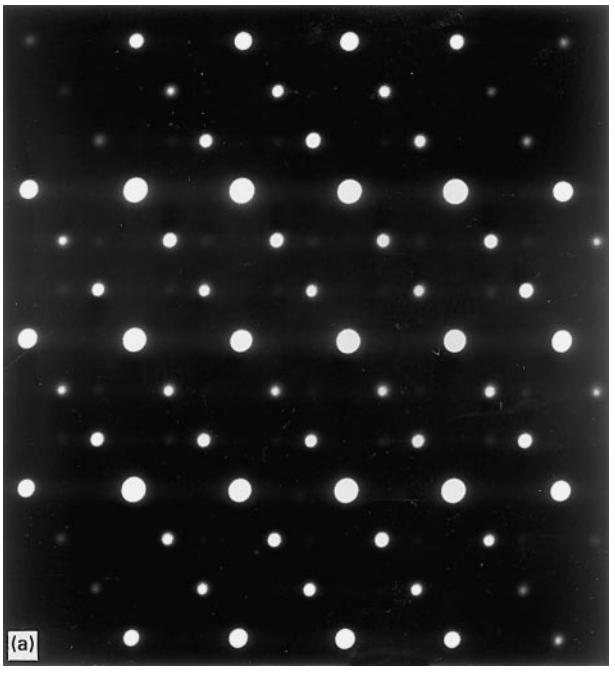

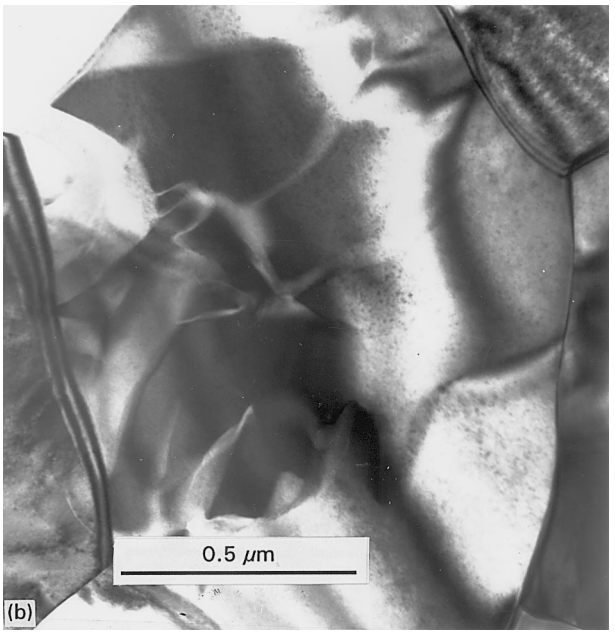

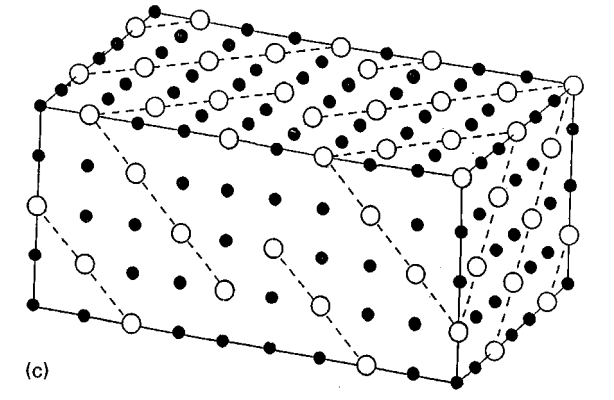

Figure 8 (a) $\langle 1\,1\,\bar{2}\,3\rangle$ zone axis diffraction pattern from BMT16 showing the presence of only one orientational variant, (b) micrograph of a grain containing predominantly antiphase boundaries (translational APBs) in BMT16, (c) diagram to show the idealized structure of an APB in a 1 : 2 ordered compound (only B-site atoms are shown).

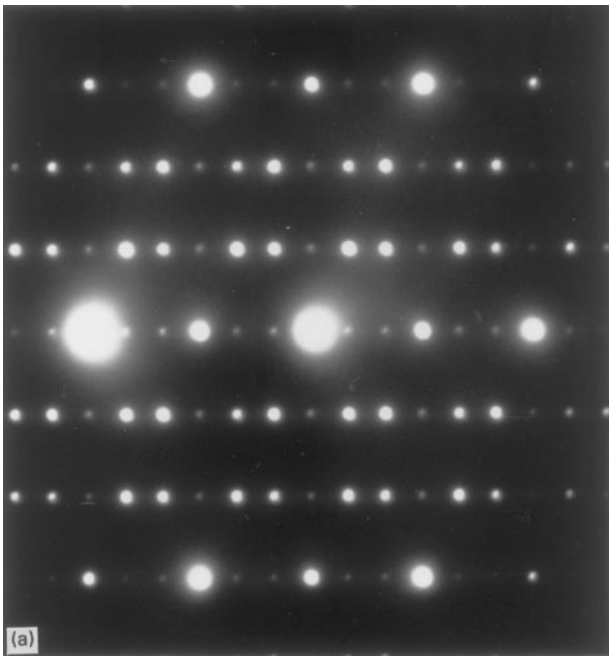

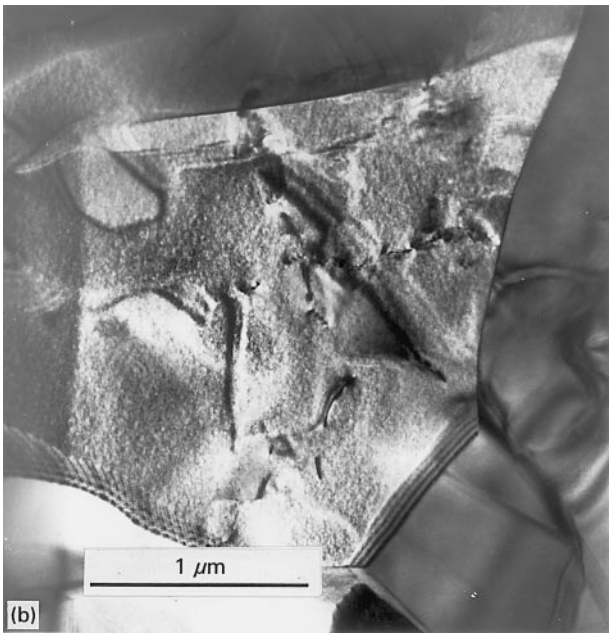

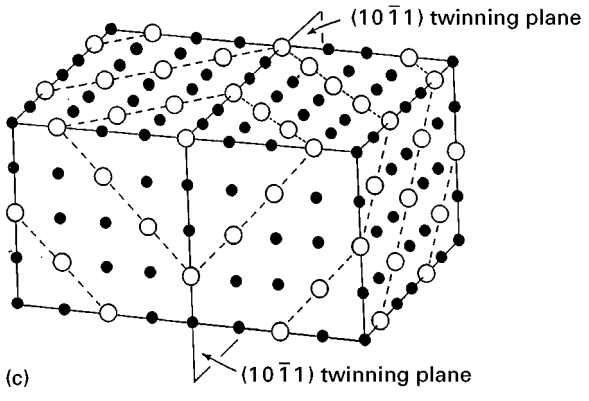

Figure 9 (a) $\langle 0\,1\,\bar{1}\,1 \rangle$ zone axis diffraction pattern from BMT16 showing the presence of twin-related orientational variants, (b) micrograph of a grain containing predominantly twin boundaries (ordering TBs) in BMT16, (c) diagram to show the idealized structure of a TB in a 1:2 ordered compound (only B-site atoms are shown).

6.4. Local inhomogeneities in the state of order

6.4.1. Grain-boundary effects

The occurrence of domains at grain peripheries which are larger than those in the grain interiors has been found previously in oxides such as the perovskite-structured ferroelectric lead, scandium tantalate, PST. Similar effects were found for PST near other types of interface [29] and were attributed to enhanced numbers of point defects facilitating the ordering process. Anomalously large domains were observed adjacent to many grain boundaries in the more completely sintered specimens. Fig. 10a shows a narrow band of larger than average domains next to a grain boundary in BZT15. The APBs typically are oriented perpendicular to the grain boundary.

6.4.2. Intragranular effects

In BMT, BZT and BZN we found small volumes with smaller than average domains (even tending to complete disorder), sometimes surrounded by larger than average domains, but more often within grains whose degree of order was typical of the whole sample. In most cases, the less-ordered area, seen in projection by TEM, was associated with at least one dislocation (we suspect that for the few exceptions the ion-milling process had removed a dislocation from either just above or below the thinned area). Fig. 10b shows a region of reduced order in BZT15. The SAD from the less-ordered region, Fig. 10c shows that it has weak 1:1 order, while SADs from the surrounding areas point to 1:2 order, Fig. 10d. X-ray microanalyses produced no clear explanation, although the less-ordered region showed a small peak apparently due to zirconium, which probably arose from a contaminant powder particle in the original compact. Fig. 10e shows a rare example of larger domain sizes associated with a wall of dislocations for the case of BZT. Microanalyses with a 50 nm probe size were carried out in the many regions of reduced order which we observed and the results were compared with microanalyses taken from the uniformly ordered regions of the same grains. The results invariably showed small differences in composition, with the more-ordered regions being essentially stoichiometric and the enclosed regions of reduced order being off stoichiometry. A systematic pattern to these deviations from stoichiometry was not discernible. The oxygen content showed the greatest variations but it could be either an excess or a deficiency (microanalyses of oxygen tend to be unreliable and we prefer to draw no conclusion). Smaller statistically significant variations in the A-site atom to the B-site atom ratios were detectable, and it appears that the B-site elements were the primary cause.

The correspondence between dislocations and local variations of the order parameter is too common to be coincidental. There is also a marked tendency for greater complexity of APB configurations when grains contain residual dislocations after sintering. The configurations do not seem to indicate that dislocations are effective nuclei for the nucleation of order, because

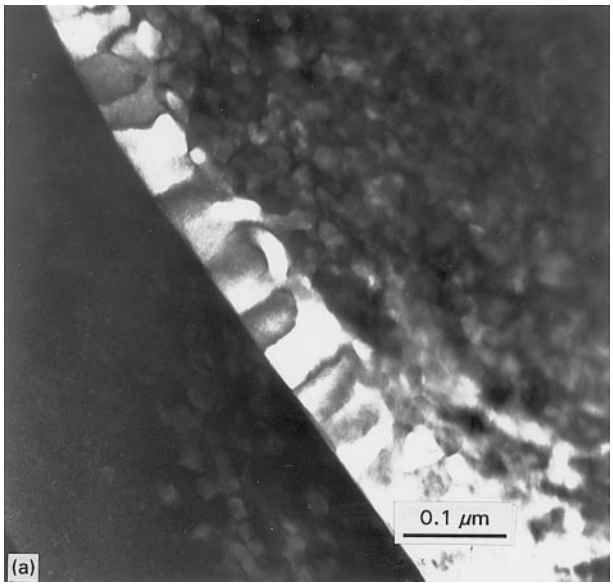

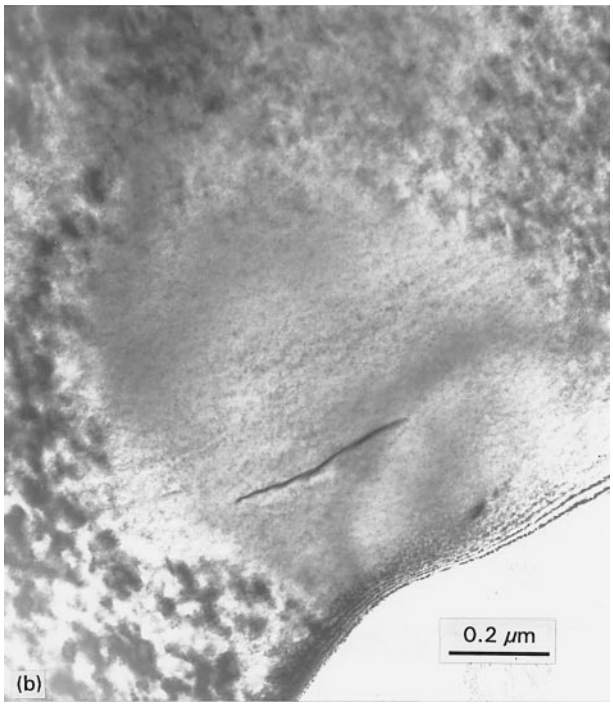

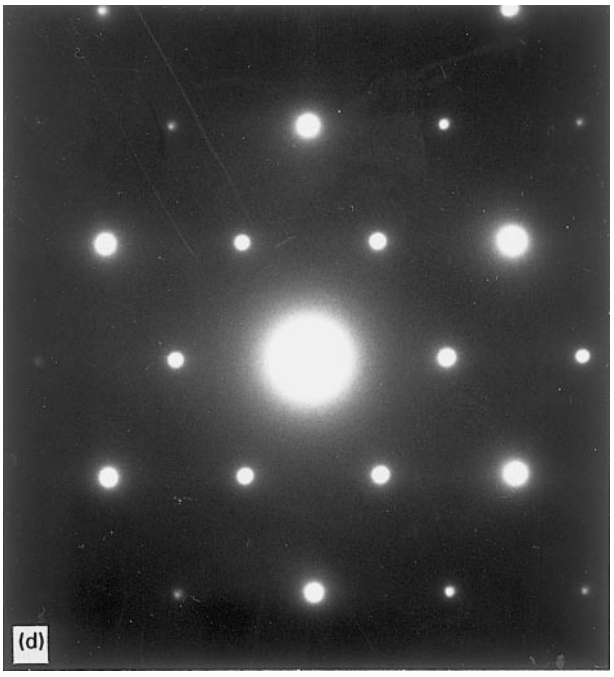

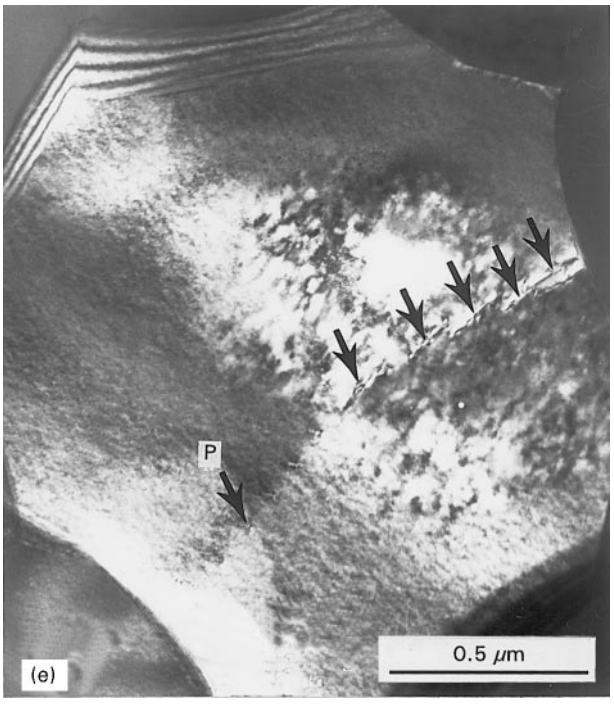

Figure 10 Dark-field micrograph taken with a superlattice reflection showing large 1 : 2 ordered domains adjacent to a grain boundary in BZT15, (b) micrograph showing a region containing domains of 1 : 1 order adjacent to a dislocation within a grain which has predominantly 1 : 2 order, (c) SAD from the 1 : 1 ordered region, (d) SAD from the 1 : 2 ordered area surrounding the 1 : 1 region, (e) micrograph showing a region with anomalously large 1 : 2 domains and which contains a wall of dislocations in BZT15 (the dislocations are slightly inclined to the electron beam where there are several arrows, and parallel to it where there is a single arrow).

the dislocations would then be in contact with larger-than-average domains, which is not observed; in fact, adjacent domains tended to be smaller. We interpret the observations as indicating that pipe diffusion causes dislocations to influence the local composition, and usually adversely. Their environs can be maintained off-stoichiometry after most of the grain structure is well equilibrated and stoichiometric. This is

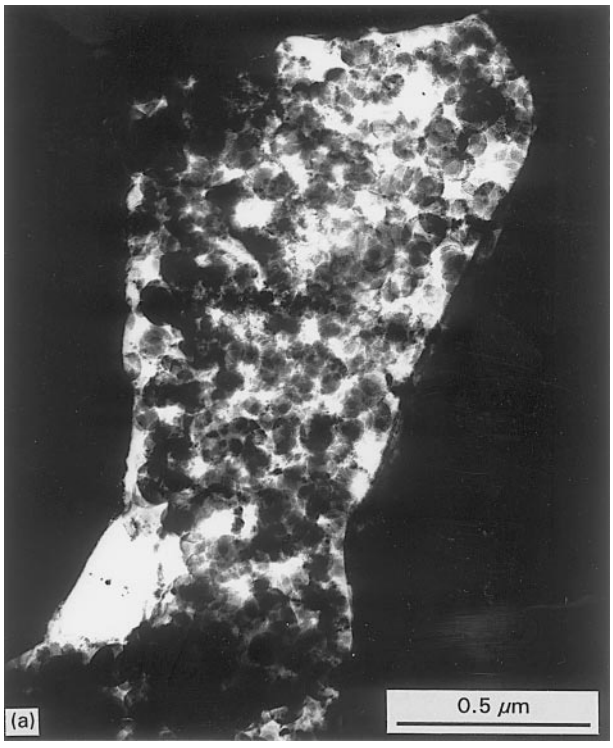

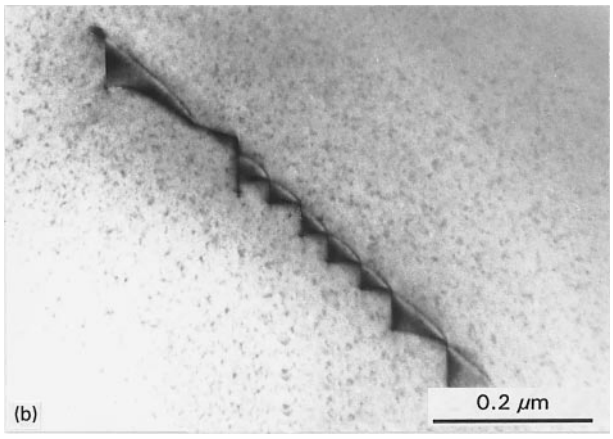

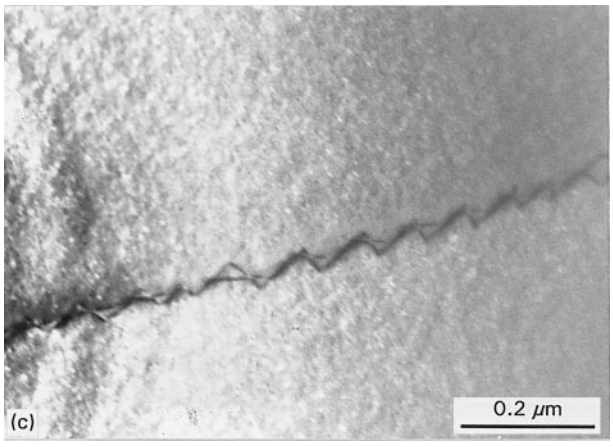

Figure 11 Micrographs showing (a) a pocket of unsintered mixed powder grains in BZN13, (b) a dislocation that has climbed and dissociated in a grain of BZN15, (c) the stacking fault contrast of another dislocation in BZN15 that has climbed and dissociated, (d) a typical core/shell grain microstructure in BMT16.

because dislocations act as conduits to grain boundaries and hence to nearby pockets of partially reacted constituents, which may persist for a time in ceramics formed by the sintering of dry oxide powders, as exemplified by Fig. 11a. Solitary super-dislocations which survive in grains that become uniformly ordered are often dissociated, also mostly showing complex effects due to climb. Fig. 11b and c are interesting because they show such effects in BZN15, which is essentially disordered. It appears that the dislocations climbed and dissociated when the material was in the partially ordered state and that the dislocation configurations became frozen when disorder set in. These split dislocations show stacking fault contrast for certain reflections. Some segments of them are even decorated with precipitates, arrowed in Fig. 11c, presumably because they have become isolated and unable to discharge any atoms in excess of stoichiometry.

Various types of "core–shell" grain structures have been reported in electrical ceramics; these are often two-phase, (e.g. [30, 31]). Another variety occurs in a minority of grains in BMT sintered at the higher temperatures. The shell mainly takes a form which is free from microstructure apart from a few radial APBs. The grain centres have distinct, irregular cores which are concentrations of various defects, including pores, dislocations linking them, occasionally second phase, and APBs separating relatively small ordered domains. An example is shown in Fig. 11d. In a small fraction of cases, the degree of order differed within a grain, being less in the core, as judged by domain sizes.

7. Discussion

The findings reported in Section 6.2 indicate that short-range and incipient long-range 1 : 1 order can occur in grains of BZN and BZT. Electron diffraction evidence of similar 1 : 1 ordering in BZN has also been reported by Harmer *et al.* [32], who found that the

intensity of the corresponding order reflections could be increased by altering the ratio of the B-site ions so as to favour 1:1 ordering. We note that the diffuse streaked intensity through the $\{h \pm \frac{1}{2}, k \pm \frac{1}{2}, l \pm \frac{1}{2}\}$ positions for BZN14 tends to shift to the $\{h \pm \frac{1}{3}, k \pm \frac{1}{3}, l \pm \frac{1}{3}\}$ positions for BZN15. We interpret this as showing that as uniform formula stoichiometry is approached during the sintering of BZN, 1:1 SRO tends to 1:2 SRO before disorder is re-established. These ideas are consistent with the results of the microanalysis of such 1:1 ordered grains and the diffraction evidence from other grains of transitional states of order.

The evidence for 1:1 order in BZT is potentially problematic because the observed diffracted intensity at $\{h \pm \frac{1}{2}, k \pm \frac{1}{2}, l \pm \frac{1}{2}\}$ positions could arise from oxygen-cage tilting. (BZN, with a tolerance factor of 1.03, should not suffer from such tilting [24].) This ambiguity is lessened by our observations on BZT that the intensity did not change as specimen temperature was decreased, as expected for scattering due to oxygen-cage tilting. Another argument is that oxygen-cage tilting would be present and indeed should occur more widely in the stoichiometric grains of well-sintered samples. This is not supported by our results and thus we favour short-range 1:1 order as the origin of the $\{h \pm \frac{1}{2}, k \pm \frac{1}{2}, l \pm \frac{1}{2}\}$ intensities. The 1:1 SRO which we find in BZT seems to be promoted by low-temperature sintering and becomes less favoured by heat treatment at higher temperatures. For the higher temperatures, 1:2 LRO mostly develops steadily as annealing proceeds until large domains are formed. However, small volumes of 1:1 order may persist within 1:2 ordered grains due to impurities or local non-stoichiometry.

The ordering transformation is somewhat simpler in BMT; there is only minimal evidence of 1:1 ordering and, when it does occur, it is only short range. Its rarity probably shows that it is only possible when there is a high local degree of non-stoichiometry. The 1:2 ordering (LRO) is ubiquitous for BMT at the lowest sintering temperatures used; both the X-ray and TEM results show that it evolves steadily. Domain sizes show large variations in partially sintered samples, apparently because of grain-to-grain and intragranular variations in composition and stoichiometry. These variations are largely eliminated in the well-sintered samples. It is interesting to note that Lu and Tsai [33] have recently linked Ba content in BMT with degree of order, finding that excess Ba favours disorder and also hinders sintering.

The explanation for anomalously large domains close to grain boundaries in BMT, illustrated in Section 6.4.1, could be simply that grain boundaries facilitate the ordering kinetics because of enhanced local diffusivity, leading to the easier achievement of stoichiometry in complex $A(B'B'')O_3$ oxides, a view that has been expressed previously. However, similar domain configurations occur in rapidly solidified intermetallic systems (e.g. [34]), with the APBs approximately normal to the boundaries. Such configurations are certainly related to grain growth. The variations in type of order and of domain sizes in BZN13 (Fig. 4a) are also interesting. We observe a correlation of domain size with grain size and often find larger domains in the proximity of grain boundaries, generally with smaller more uniform domains at grain interiors. This appears to indicate that both diffusion and grain-boundary migration at this temperature have marked effects on the ordering process.

Finer domain sizes in grain interiors in metal alloys are usually attributed to deviations from ideal composition caused by solute partitioning. Despite this interpretation, there is clear evidence in some metallic systems [35] that advancing grain boundaries cause heterogeneous ordering at temperatures too low to favour homogeneous ordering, causing anomalously large domains to form behind the grain boundaries. From our results it appears that in oxides too the grain boundaries play a more active role than simply one of stimulating ordering by means of increased local diffusivity. The observations in Section 6.4.2 lend support to the view that the domain size is strongly affected by grain-boundary migration during sintering.

Both grain boundaries and dislocations can enhance the local diffusivity, and we note their effects on the ordering process. Grain boundaries tend to be associated with anomalously large domains (i.e. well-ordered material). Dislocations are almost always to be found where there are local variations in domain size in incompletely sintered samples. They are mostly associated with regions of reduced order, thus tending to give the opposite effect to grain boundaries. We have already concluded that the transversely elongated domains or anomalously large domains next to grain boundaries are formed during grain-boundary advance with enhanced diffusion. They indicate that ordering is concurrent with sintering, which is consistent with our observations that order is present in many grains while gross compositional inhomogeneities still exist within the compact. As the constituents of pockets of incompletely reacted powders disperse they can either favour or arrest ordering through changes in local composition, and may even promote disordering by causing temporary deviations away from stoichiometry. (This appears to be the explanation for the occurrence but relative instability of 1:1 order in BZN and BZT.) The volume surrounding a dislocation can continue to be off-stoichiometry when the bulk of a grain is stoichiometric, and then ordering is impeded. As stoichiometry is approached, such dislocations tend both to climb and to dissociate. The finding of frozen-in dissociated dislocations in the disordered BZN is surprising and indicates that our understanding of the order/disorder behaviour of this material is still incomplete.

The finding of grains of MgO in all BMT samples appears to be previously unreported. Although their presence seems to suggest that the BMT cannot be exactly stoichiometric, any effects of the grains on ordering are not apparent; there are no visible local inhomogeneities in order. The ease of formation or persistence of MgO in BMT will influence the dielectric loss, however, and may contribute to the reported variation of loss as a function of sintering temperature. The tendency for core–mantle structures to develop

during sintering is also relevant to the dielectric properties whose optimization will be prevented if a significant proportion of grains contain such inhomogeneities.

Viewed overall, our results identify several factors that can affect the state of order and its uniformity and, in turn, that will influence the microwave dielectric properties of the compounds studied. The different ways in which ordering proceeds in the three compounds reinforces the unexceptional conclusion that processing conditions must be optimized for each one and that there can be no universal recipe. The effects of partially or unreacted starting materials should not be discounted. Newer fabrication methods can consistently achieve homogeneously mixed precursors (e.g. sol–gel routes) at the nanoscale. These have the potential to produce better quality materials and more uniform ordering. In such systems, which are applicable to the three compounds we have studied (e.g. [36]), there is the potential to tailor physical properties closely by controlling of the type and degree of order through chemical composition.

Acknowledgements

We thank Professor Rongrun Lu, Institute of Radio Metrology and Measurement, Beijing, for his help in making the dielectric measurements, and Dr I. M. Reaney, Sheffield University, UK, for helpful comments on the draft manuscript. We gratefully acknowledge access to equipment in the Materials Characterisation and Preparation Centre, Hong Kong University of Science and Technology, and financial support (HKUST119/92E) from the University Grants Council of Hong Kong.

References

1. F. GALASSO, L. KATZ and R. WARD, *J. Amer. Chem. Soc.* **82** (1959) 820.
2. F. GALASSO and J. PYLE, *Inorg. Chem.* **2** (1963) 482.
3. *Idem*, *J. Phys. Chem.* **67** (1963) 1563.
4. F. GALASSO and J. PINTO, *Nature* **207** (1965) 70.
5. F. GALASSO, J. R. BARRANTE and L. KATZ, *J. Amer. Chem. Soc.* **83** (1961) 2830.
6. S. KAWASHIMA, M. NISHIDA, I. UEDA and H. OUCHI, *ibid.* **66** (1983) 421.
7. S. NOMURA, K. TOYAMA and K. KANETA, *Jpn. J. Appl. Phys.* **21** (1982) L624.
8. S. B. DESU and H. M. O'BRYAN, *J. Amer. Ceram. Soc.* **68** (1985) 546.
9. K. MATSUMOTO, T. HIUGA, K. TAKADA and H. ICHIMURA, in "*Proceedings of the 6th IEEE International Symposium on Ferroelectrics*" (ISAF '86), Bethlehem, 1986. Edited by V. E. Wood (IEEE Publishing Services, New York, 1986) p. 118.
10. T. FUKUI, C. SAKURAI and M. OKUYAMA, *J. Mater. Res.* **7** (1992) 1883.
11. D. A. SAGALA and S. NAMBU, *J. Amer. Ceram. Soc.* **75** (1992) 2573.
12. N. SETTER and L. E. CROSS, *J. Mater. Sci.* **15** (1980) 2478.
13. H. M. CHAN, M. P. HARMER, A. BHALLA and L. E. CROSS, *Jpn. J. Appl. Phys.* **24** (1985) 550.
14. C. A. RANDALL, D. J. BARBER, R. W. WHATMORE and P. GROVES, *J. Mater. Sci.* **21** (1986) 4456.
15. C. A. RANDALL, D. J. BARBER, P. GROVES and R. W. WHATMORE, *ibid.* **23** (1988) 3678.
16. R. S. IRANI, *Contemp. Phys.* **13** (1972) 559.
17. C. A. RANDALL, A. S. BHALLA, T. R. SHROUT and L. E. CROSS, *Ferroelectrics Lett.* **11** (1990) 103.
18. A. D. HILTON, D. J. BARBER, C. A. RANDALL and T. A. SHROUT, *J. Mater. Sci.* **25** (1990) 3461
19. J. CHEN, H. M. CHAN and M. P. HARMER, *J. Amer. Ceram. Soc.* **72** (1989) 593.
20. T. A. SHROUT, W. HUEBNER, C. A. RANDALL and A. D. HILTON, *Ferroelectrics* **93** (1989) 961.
21. G. VAN TENDELOO, in "Alloy Phase Stability" edited by G. M. Stocks and A. Gonis, *NATO ISI Series E*: *Applied Sciences*, Vol. **163** (1987) p. 75.
22. A. M. GLAZER, *Acta Crystallogr.* **B28** (1972) 3384.
23. *Idem*, *ibid.* **A31** (1975) 756.
24. I. M. REANEY, E. L. COLLA and N. SETTER, *Jpn J. Appl. Phys.* **33** (1994) 3984.
25. H. MEGAW, *Proc. Phys. Soc.* **58** (1946) 133.
26. E. L. COLLA, I. M. REANEY and N. SETTER, *Ferroelectrics* **133** (1992) 217.
27. *Idem*, *J. Appl. Phys.* **74** (1993) 3414.
28. E. S. KIM and K. H. YOON, *Ferroelectrics* **133** (1992) 187.
29. I. M. REANEY, D. J. BARBER and R. WATTON, *J. Mater. Sci. Mater. Electron.* **3** (1992) 51.
30. D. HENNINGS and G. ROSENSTEIN, *J. Amer. Ceram. Soc.* **67** (1984) 249.
31. C. SAUCY, I. M. REANEY and A. J. BELL, *Br. Ceram. Soc. Proc.* **49** (1992) 31.
32. M. P. HARMER, J. CHEN, P. PENG, H. M. CHAN and D. M. SMYTH, *Ferroelectrics* **97** (1989) 263.
33. C.-H. LU and C.-C. TSAI, *J. Mater. Res.*, **11** (1996) 1219.
34. D. G. MORRIS, in "Ordered Intermetallics – Physical Metallurgy and Mechanical Behaviour", edited by C. T. Liu, R. W. Cahn and G. Sauthoff NATO ISI Series E, Vol. **213** (Kluwer Academic, Dordrecht, The Netherlands, 1992) p. 123.
35. M. RAJKOVIC and R. A. BUCKLEY, *Metal Sci.* **15** (1981) 21.
36. O. RENOULT, J.-P. BOILOT, F. CHAPUT, R. PAPIERNIK, L. G. HUBERT-PFALZGRAF and M. LEJEUNE, *J. Amer. Ceram. Soc.* **75** (1992) 3337.

Received 20 November 1995
and accepted 15 January 1996